Available online at www.sciencedirect.com
ScienceDirect
Journal of Power Sources 164 (2007) 868–873
JOURNAL OF POWER SOURCES
www.elsevier.com/locate/jpowsour

Short communication

Phase formation and electrochemical properties of cryochemically processed $Li_{1+x}V_3O_8$ materials

Oleg A. Brylev [a], Oleg A. Shlyakhtin [a,b,*,1], Alexander V. Egorov [a], Yuri D. Tretyakov [a,c]

[a] *Department of Chemistry, Moscow State University, Vorob'evy Hills, Moscow 119992, Russia*
[b] *Institute of Chemical Physics, Russian Academy of Sciences, Moscow 119991, Russia*
[c] *Department of Materials Science, Moscow State University, Vorob'evy Hills, Moscow 119992, Russia*

Received 19 July 2006; received in revised form 19 October 2006; accepted 23 October 2006
Available online 8 December 2006

Abstract

$Li_{1+x}V_3O_8$ cathode materials for secondary Li batteries are prepared by freeze drying (FD) synthesis from aqueous solutions of NH_4VO_3 and various Li salts at different pH values. The polyanionic forms of vanadates in the FD products are significantly different from the ones existing in the starting solutions. The degree of VO_3^- polymerization is influenced both by co-existing anion and by pH value of the starting solution. The appearance of $NH_4V_3O_8$ among FD products promotes a faster formation of the crystallochemically similar LiV_3O_8 during the following solid state metathesis reaction. LiV_3O_8 powders obtained by the thermal decomposition of various FD precursors at 300–400 °C demonstrate rather different micromorphologies and drastically dissimilar electrochemical properties. The best electrochemical performance is exhibited by poorly crystalline but faceted fine particles obtained by the thermal decomposition of nitrate-containing precursor.

Keywords: Secondary Li batteries; Cathode materials; $Li_{1+x}V_3O_8$; Freeze drying; Particle morphology

1. Introduction

$Li_{1+y}V_3O_8$ ($y \approx 0.2$) is a lithium vanadium bronze considered as one of promising cathode materials for rechargeable lithium batteries due to its low cost, high electronic conductivity and potentially high specific electrochemical capacity [1,2]. It is known that upon Li uptake (x) $Li_{1+x}V_3O_8$ undergoes structural modifications accompanied by a second-order phase transition from the low-lithiated form (ca. $Li_{2.9}V_3O_8$) into the high-lithiated one (ca. $Li_4V_3O_8$) [3,4]. Accordingly, the process of Li electrochemical intercalation into $Li_{1+y}V_3O_8$ can be divided into three steps: single phase Li intercalation into low-lithiated phase, coexistence of the two phases ($1.9 < x < 3.0$) and single phase Li intercalation into $Li_4V_3O_8$ [5]. Due to the structural difference between the two forms of $Li_{1+x}V_3O_8$ the lithium insertion process is not totally reversible; a little alteration of the initial structure after repetitive electrochemical cycling was observed [6]. It was also shown that the transformation of $Li_{1+x}V_3O_8$ from one structural type to the other one can occur at different x values [5,6]. Another important feature of the Li intercalation process is a significant decrease in Li^+ diffusion rate at high Li content [7]. All these factors point to the crucial influence of kinetic factors on the lithium diffusion and, hence, to the completely different electrochemical performance of $Li_{1+x}V_3O_8$ materials obtained by different methods.

The traditional methods of $Li_{1+y}V_3O_8$ synthesis are based on the slow cooling of melt, obtained from V_2O_5 and Li_2CO_3 at 680–900 °C [8–10]. This preparation route leads to the reproducible formation of perfectly crystalline faceted $Li_{1+y}V_3O_8$ particles; amorphous quenching products demonstrated a much poorer electrochemical capacity. However, due to the large grain size and above-mentioned kinetic complications of Li^+ mobility at high x values these materials usually demonstrate a moderate

* Corresponding author at: Institute of Chemical Physics, Russian Academy of Sciences, Moscow 119991, Russia.
E-mail addresses: oleg@inorg.chem.msu.ru, oleg@kist.re.kr (O.A. Shlyakhtin).
[1] Present address: Thin Film Materials Research Center, Korea Institute of Science and Technology, 39-1 Hawolgok-dong, Seongbuk-gu, 136-791 Seoul, Korea. Tel.: +82 2 958 5554; fax: +82 2 958 5554.

0378-7753/$ – see front matter © 2006 Elsevier B.V. All rights reserved.
doi:10.1016/j.jpowsour.2006.10.066

electrochemical capacity (<180 mAh g^{-1}) often accompanied by a high fade rate.

The most of modern $Li_{1+x}V_3O_8$ studies deal with the chemical methods of powder synthesis. The decrease in particle size diminishes Li^+ diffusion pathways, and thus ensuring a better electrochemical performance [7]. It was shown that the soft dehydration of the gel obtained by dissolution of V_2O_5 in the aqueous LiOH results in the formation of poorly crystalline product with individual structure, identified as polymorph of LiV_3O_8 [11] or $LiV_3O_8{\cdot}(H_2O)_z$ [12], that can accommodate over 4 Li per formula unit [11,13]. Usually the highest initial specific capacity values (>300 mAh g^{-1}) are demonstrated by the $Li_{1+x}V_3O_8$ materials with ordinary monoclinic structure of the γ-lithium vanadate [3] obtained by the thermal processing of various precursors at 300–400 °C, though an important capacity fade rate upon cycling is often observed [14,15]. Thermal processing performed below 300 °C is usually insufficient for the complete removal of intermediate decomposition products while the increase in thermal processing temperature over 400 °C causes the progressive degradation of electrochemical performance [16–18], that can be attributed to the intensive grain growth and related kinetic complications of Li^+ diffusion.

Different synthesis methods lead to substantially different $Li_{1+x}V_3O_8$ crystallization rates, so that the crystallinity degree of powders, obtained at 300–400 °C, is rather different; particle size, morphology and packing are also strongly influenced by synthesis routes [19–22]. However, the electrochemical performance of almost amorphous and well-crystallized powders obtained in this temperature range is often very similar and close to 250–270 mAh g^{-1} at a moderate discharge rate [14,17,18,21].

Meanwhile, the considerable discrepancy of results obtained by various authors clearly demonstrates that numerous factors controlling the electrochemical behavior of $Li_{1+x}V_3O_8$ fine powders still have to be revealed. Taking account of restrained information concerning the influence of chemical prehistory on the properties of $Li_{1+x}V_3O_8$-based cathode materials and the versatility of cryochemical processing methods [23], this study is devoted to the freeze-drying synthesis of $Li_{1+x}V_3O_8$ powders from different salt precursors and to the investigation of the phase formation, microstructure and electrochemical properties of the final materials.

2. Experimental

The most of LiV_3O_8 materials in the present study were prepared from the $LiNO_3{\cdot}H_2O$ (Aldrich, 98%) + NH_4VO_3 (Aldrich, 99+%) precursor (further denoted as LV1). Several experiments were performed using $CH_3COOLi{\cdot}2H_2O$ (Aldrich, 99.999%) + NH_4VO_3 (LV2) and $HCOOLi{\cdot}H_2O$ (Aldrich, 98+%) + NH_4VO_3 (LV3) precursors. Aqueous solutions containing Li and V salts in molar ratio 1.2:3 were sprayed into liquid nitrogen by pneumatic nozzle and freeze dried at 5×10^{-2} mbar for 48 h at $T \leq 42$ °C. The pH of the starting solution was adjusted to a necessary value by adding either NH_3(aq) or a corresponding acid. In order to clarify the impact of freeze-drying on thermal decomposition and phase formation processes, the same precursors were prepared by mechanical mixing of the same salts in the same Li/V ratio (1.2/3). As-obtained precursors were heated at 5 °C min^{-1} until dwelling temperature (300–500 °C) and held for 6 h.

Thermal analysis (TG and DSC/DTA) was performed in air in a 20–600 °C temperature range at a heating rate 5 °C min^{-1} (STA 409 Netsch). XRD analysis was carried out on Siemens D5000 diffractometer equipped with a secondary graphite monochromator in the 10–80° 2Θ range (step 0.04°, acquisition time 6 s). SEM measurements were performed using Jeol JSM-35 microscope (accelerating voltage 15 kV, 50–30,000× magnification).

For the electrochemical experiments a CA2430 coin type cell was used. The negative electrode was a lithium foil disk. The composite cathodes consisted of 80% of $Li_{1.2}V_3O_8$, 15% of polyvinylidene difluoride (Kynar Flex 282, Elf Atochem) and 5% of acetylene black. The preparation of electrolyte (1 M $LiClO_4$ solution in the mixture of EC:PC:DME = 1:2:2) and coin cell assembling was carried out in an argon glove box with the water vapor and oxygen content less than 1 ppm. Preliminarily the utilized organic solvents were dried on molecular sieve, and $LiClO_4$ powder (p.A., 99%, Acros Organics) was dehydrated in vacuum at 150 °C. The water content in the electrolyte, determined by K. Fischer coulometry, did not exceed 10 ppm. The microporous film Celgard 2400 was used as a separator. A macroporous film Viledon™ was placed between a lithium disk and microporous separator for a better impregnation of different components of the battery during functioning.

Electrochemical measurements were performed at 25 °C with two-electrode coin cells on a battery cycler (Arbin Instruments, TX, USA) under galvanostatic conditions, at C/30, C/10, C/5 and C/2 rates in the voltage range 1.2–3.8 V versus Li/Li^+. Open circuit voltage (OCV) measurements were performed at 25 °C with three-electrode coin cells on a potentiostat–galvanostat MacPile (CNRS, Grenoble) operated by the program MacPile A-3.22 (Bio-Logic, Claix).

3. Results and discussion

The phase composition of freeze dried salt precursors is one of the key factors controlling the formation mechanism and morphology of the freeze drying synthesis products [23]. Indeed, XRD patterns of the LiV_3O_8 precursors obtained from starting solutions with different anionic compositions were found considerably different. All the freeze-dried precursors contained various polyvanadates while LV2 and LV3 precursors contained also hydrated lithium acetate and formate, respectively. In LV1 the lithium nitrate remained amorphous irrespectively of pH value, though the appearance of ammonium nitrate, which was absent in the starting solution, was detected.

Another important parameter affecting the phase composition of FD powders is the pH value of starting solution. It is known that the appearance and the ratio of polyvanadate ions in aqueous solutions greatly depend on the pH value and the concentration of solution; for example, lower pH values promote the polymerization of VO_3^- [24,25]. The comparison of literature data with XRD patterns of obtained FD products demonstrates the absence of direct correlations between the predicted polymeriza-

tion degree of VO_3^- anion in the aqueous medium and vanadate forms observed in FD precursors. This is also the case for the lithium-free solution of ammonium metavanadate subjected to freeze-drying. At pH > 8 the only product of freeze-drying was NH_4VO_3, while at pH 3–4 the presence of various polyvanadate ions was detected.

For LV1 precursor obtained at pH 3 $NH_4VO_3{\cdot}0.5H_2O$, $(NH_4)_{0.38}V_2O_5$ and NH_4VO_3 were detected by XRD. This phase composition is similar to the one of freeze-dried solution of NH_4VO_3 at the same pH value (Fig. 1a). At pH 8, $(NH_4)_4V_6O_{17}{\cdot}14H_2O$ and $(NH_4)_6V_{10}O_{28}{\cdot}6H_2O$ dominated in the freeze-dried powder, and in this case the compositions of freeze-dried NH_4VO_3 and LV1 solutions were substantially different (Fig. 1b). This fact confirms the influence of Li^+ cation on the polymerization degree of VO_3^- that has been already observed for other cations [24,25]. The presence of NH_4NO_3 at pH 3 can be related to the trimerization of VO_3^- into $V_3O_8^-$, accompanied by the formation of additional ammonium cations and OH^- ions, neutralized then by nitric acid.

The similarity of $NH_4V_3O_8$ and LiV_3O_8 crystal structures promotes the formation of lithium trivanadate from LV1 precursor obtained at pH 3. Due to the particularities of so-called solid

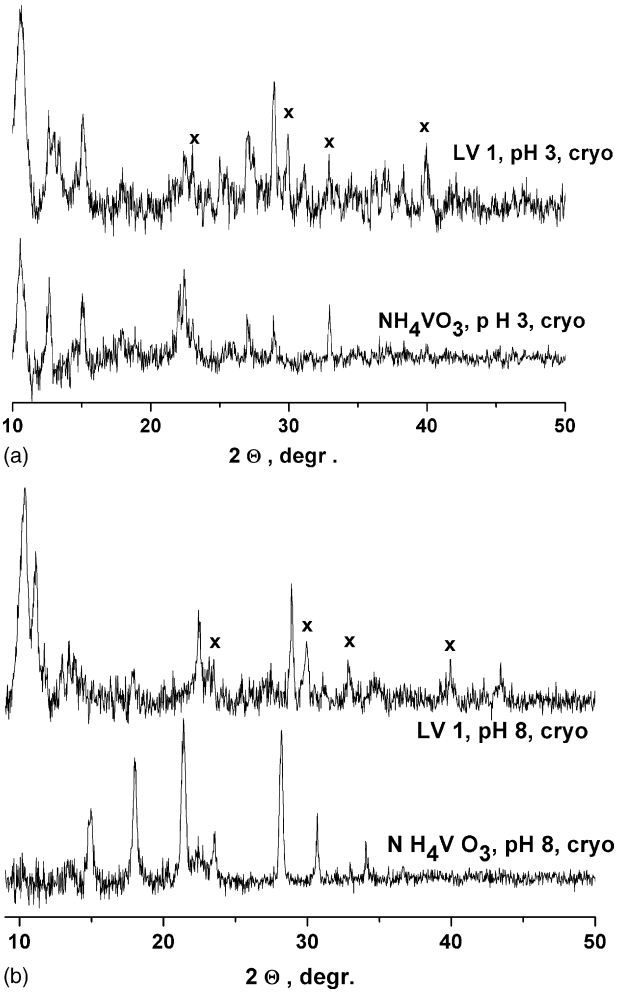

Fig. 1. XRD patterns of freeze-dried NH_4VO_3 and $LiNO_3 + NH_4VO_3$ solutions at (a) pH 3; (b) pH 8. ($x = NH_4NO_3$).

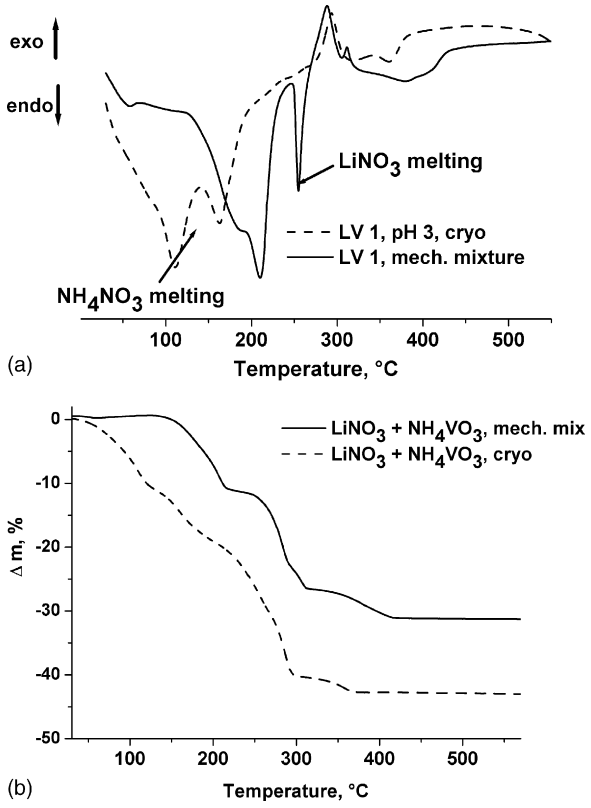

Fig. 2. (a) DTA and (b) TG curves for freeze-dried $LiNO_3 + NH_4VO_3$ precursor and mechanical mixture of $LiNO_3 + NH_4VO_3$.

state metathesis reactions [26], the melting of NH_4NO_3 which is present in the freeze-dried precursor (Fig. 2a, dashed line) drastically accelerates the $NH_4^+ \rightarrow Li^+$ solid state exchange. Accordingly in the course of thermal decomposition, lithium nitrate disappears as an individual phase. It is unambiguously confirmed by the absence of $LiNO_3$ melting peak usually observed at 253 °C (Fig. 2a, dotted line), which is however clearly present in the case of $LiNO_3$ and NH_4VO_3 mechanical mixture (Fig. 2a, solid line). For freeze-dried precursors LiV_3O_8 is mainly formed at 250–300 °C, but its formation from $(NH_4)_{0.38}V_2O_5$, which is also present in the freeze-dried precursor at pH 3, is apparently more difficult. This fact seems to be a main reason of relatively high temperature of the completion of FD precursor decomposition and LiV_3O_8 phase formation close to the ones for the mechanical mixture of $LiNO_3$ and NH_4VO_3 (Fig. 2b). It should be also pointed out that the direct comparison of phase formation processes using thermal analysis data is complicated because of small thermal effects of solid state synthesis reactions and the formation of amorphous intermediates. Indeed, XRD analysis shows that, in spite of similar end temperatures of thermal decomposition, thermal processing of the highly homogeneous LV1 precursor causes the formation of the single phase LiV_3O_8 at 300 °C (Fig. 3) while after thermal treatment of the corresponding mechanical mixture at 500 °C for 6 h, $LiVO_3$ and V_2O_5 are still identified as impurities (not shown).

As stated above, the crystallinity of LiV_3O_8 fine powders obtained by various chemical methods at similar processing

Table 1
Lattice parameters for $Li_{1.2}V_3O_8$ materials obtained at 400 °C

	LV1, pH 3	LV1, pH 4	LV2, pH 3	LV2, pH 4	LV3, pH 3	LV3, pH 4
a (Å)	6.682(3)	6.677(3)	6.684(2)	6.679(2)	6.678(2)	6.678(2)
b (Å)	3.599(1)	3.603(1)	3.600(1)	3.599(1)	3.601(1)	3.600(1)
c (Å)	12.040(4)	12.028(6)	12.028(5)	12.037(4)	12.031(3)	12.027(5)
β (°)	107.84(3)	107.74(3)	107.85(3)	107.83(2)	107.83(3)	107.78(4)

temperatures can be also very different. For LV1 precursors the intermediate products of their thermal decomposition remained amorphous until $T < 300$ °C which is evidenced by broad XRD peak at $2\Theta \approx 18°$ (Fig. 3), while the presence of $Li_{0.3}V_2O_5$ was observed in the case of LV2 and LV3 precursors. However, heat treatment at 400 °C for 6 h causes the formation of the single-phase LiV_3O_8 irrespectively of the nature of freeze-dried precursor and the pH value of starting solution. In spite of the difference in phase composition of the freeze-dried salt precursors, lattice parameters (Table 1) and IR-spectra of obtained LiV_3O_8 materials were practically the same irrespectively of the anion composition and pH of the initial aqueous solution.

Apart from crystallographic parameters, the micromorphology of LiV_3O_8 powders demonstrated an obvious dependence on their chemical prehistory. Taking account of the high anisotropy of $Li_{1+x}V_3O_8$ crystal structure and, hence, of the different orientation of lithium diffusion pathways for the materials with different morphology, the form-factor of LiV_3O_8 materials is crucial for their electrochemical properties. SEM micrographs for the LiV_3O_8 materials obtained from freeze-dried precursors at 400 °C are represented in Fig. 4. The most obvious difference is observed between LV1-derived small faceted particles (Fig. 4a) and large conglomerates with poorly resolved internal structure, obtained from LV3 precursor (Fig. 4b). The architecture of the crystallites packing – micromorphology of primary agglomerates – is also strongly influenced by the anion composition of starting solutions. Platelike crystallites of LV1-LiV_3O_8 are loosely packed so that a good contact with electrolyte is ensured for almost any particle of lithium trivanadate (Fig. 4a).

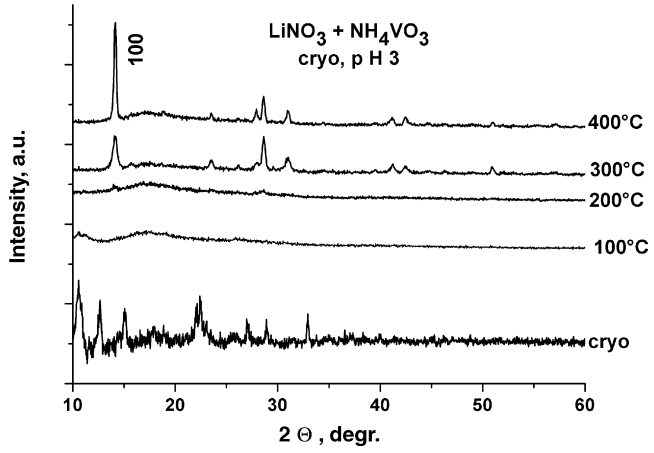

Fig. 3. XRD patterns of freeze-dried $LiNO_3 + NH_4VO_3$ (pH 3) and of the products of its thermal treatment for 6 h at different temperatures.

Needle-like crystallites of LV2-LiV_3O_8 are packed substantially closer (Fig. 4c), while LV3-LiV_3O_8 forms large dense flakes with severely reduced electrode–electrolyte interface (Fig. 4b).

Such features of the particle packing might be rather important for electrochemical cycling at high discharge rates. The initial discharge capacity values (C/10 charge–discharge rate) correspond to the intercalation of about 3 mol of Li per LiV_3O_8 formula unit (Table 2). However, the samples with the highest initial capacity values usually demonstrate a considerable fade rate during cycling, while stable and reproducible cycling behavior was observed for LV1-LiV_3O_8 samples with platelike grain morphology at capacity values ~200 mAh g^{-1} that corresponds to the upper boundary of the low-lithiated form (I) of $Li_{1+x}V_3O_8$ [24]. Similar stabilization at these capacity values was also observed in [22] for faceted LiV_3O_8 powders with platelike morphology.

Concerning OCV measurements, a plateau appears for $x = 1.4$–2.3 for all the investigated samples. It corresponds to the co-existence of low-lithiated (I) and high-lithiated (II) modifications of $Li_{1+x}V_3O_8$ [24]. It is possible to calculate the cathode polarization by the difference between the cell potential and OCV at a given lithium content. Such a dependence for LiV_3O_8 obtained from LV1 precursors at different pH values is shown in Fig. 5.

It should be pointed out that in the I → II phase transition region for $Li_{1+x}V_3O_8$ obtained at pH 3, the cathode polarization is more significant than for other materials obtained from LV1 precursors (Fig. 5). It can be resulted from the micromorphology of LiV_3O_8 particles, causing the kinetic limitations of lithium insertion. It can lead to the restrained access to favorably oriented crystallite zones, to longer lithium diffusion pathways, and, hence, to a decrease in a lithium intercalation rate which finally results in a more significant cell polarization. Due to these facts, the I → II phase transition occurs in this case rather slowly and is almost stopped during further cycling, which is confirmed by galvanostatic measurements. The capacity values for LV1-

Table 2
Specific discharge capacity (mAh g^{-1}) for the first cycle of LiV_3O_8 materials obtained from different freeze-dried precursors

Precursor composition	Synthesis conditions			
	pH 3, 300 °C	pH 3, 400 °C	pH 4, 400 °C	pH 8, 400 °C
$LiNO_3 + NH_4VO_3$	234	255	250	275
$CH_3COOLi + NH_4VO_3$	321	298	278	268
$HCOOLi + NH_4VO_3$	260	204	291	229

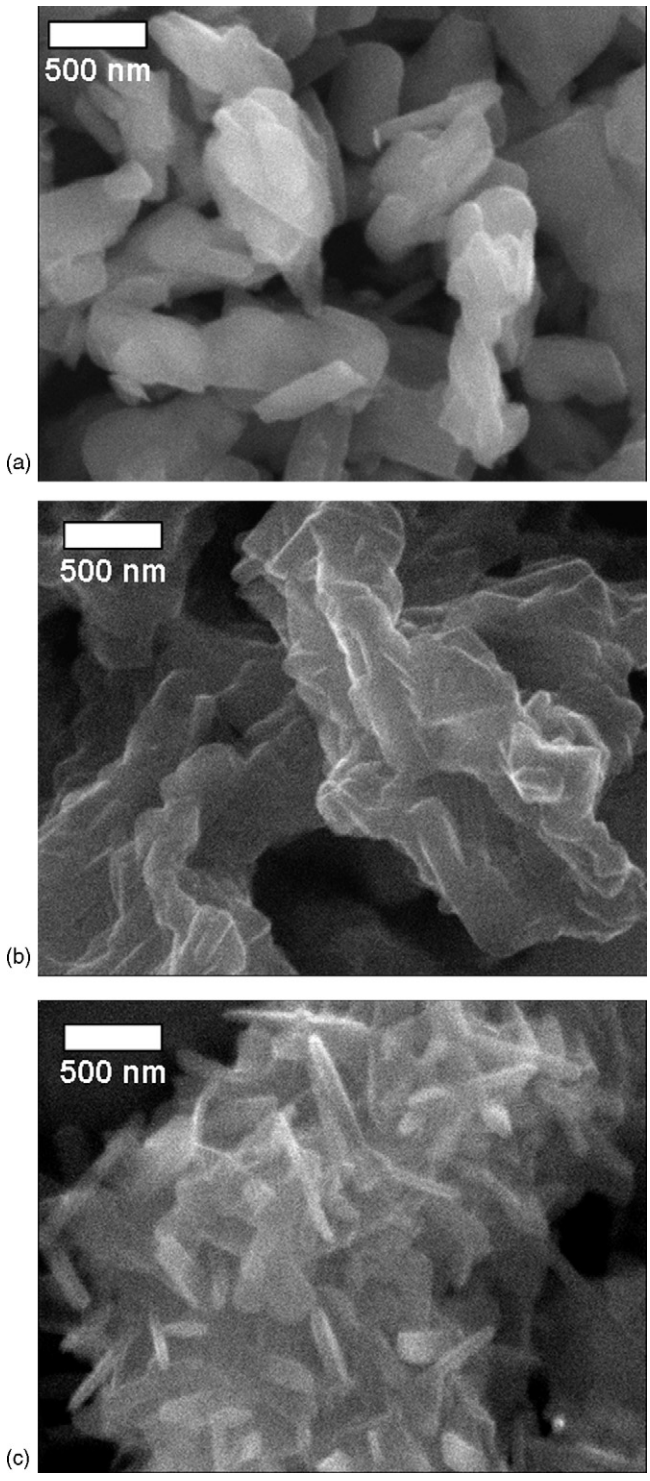

Fig. 4. SEM micrographs (magnification 30,000×) for $Li_{1.2}V_3O_8$ powders obtained at 400 °C from freeze-dried precursors at pH 3: (a) $LiNO_3 + NH_4VO_3$; (b) $HCOOLi + NH_4VO_3$; (c) $CH_3COOLi + NH_4VO_3$.

LiV_3O_8 obtained at pH 3 remain stable versus cycle number, which means that the materials can be reversibly cycled within the limits of low-lithiated modification existence (Fig. 6-1). The materials obtained from nitrate-based precursors at pH 3 also turn out to be the best in terms of rate capability compared to the materials with other anion prehistory.

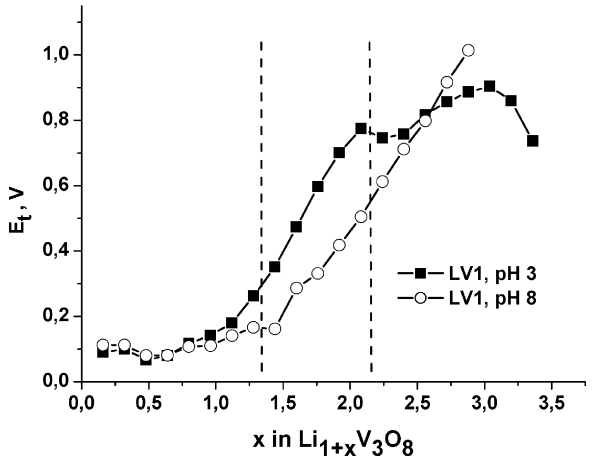

Fig. 5. Non-ohmic voltage drop of the lithium cells with LiV_3O_8 cathode synthesized from $LiNO_3 + NH_4VO_3$ (LV1) at 400 °C (pH 3 and 8).

At pH 4, the modified powder micromorphology of LV1-derived materials facilitates the lithium transport that results in decreasing the cell polarization. It shows that in this case the phase transition is not so much complicated. Upon cycling, the rearrangement of crystallographic domains, caused by phase transition, promotes blocking the lithium diffusion pathways.

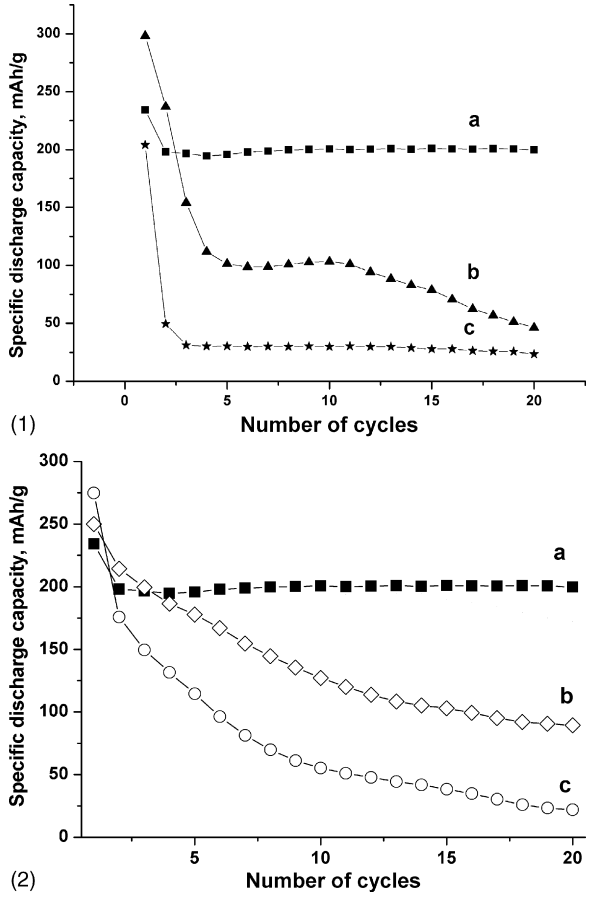

Fig. 6. Specific discharge capacity vs. cycle number for LiV_3O_8 materials obtained from (1) a, $LiNO_3 + NH_4VO_3$; b, $CH3COOLi + NH_4VO_3$; c, $HCOOLi + NH_4VO_3$. (2) From $LiNO_3 + NH_4VO_3$, annealed at 400 °C for: a, pH 3; b, pH 4; c, pH 8.

Such a rearrangement proceeds even more easily for the LV1-LiV_3O_8 obtained at pH 8 (Fig. 5) that promotes a rapid decrease in discharge capacity observed upon cycling at pH > 3 (Fig. 6-2). Concerning the materials obtained from acetate and formate precursors, the particle morphology also seems to be the key factor controlling their electrochemical performance.

4. Conclusions

The freeze drying of aqueous solutions containing NH_4VO_3 and various Li compounds results in the formation of salt precursors containing polyvanadate anions which considerably differ from those existing in aqueous medium. The decrease in the pH of starting solution promotes the formation of $NH_4V_3O_8$, which is crystallographically similar to LiV_3O_8. Thus, its formation is facilitated during the thermolysis, and the thermal decomposition of freeze dried precursors results in the formation of LiV_3O_8 at $T > 300\,^{\circ}C$. The powders obtained from different precursors are poorly distinguishable by their crystallographic parameters and IR spectra, while their micromorphology and electrochemical performance are rather different. The best electrochemical cyclability is demonstrated by the fine, faceted and loosely agglomerated LiV_3O_8 powders, obtained from freeze dried $LiNO_3 + NH_4VO_3$ solution at 400 °C. Better capacity retention for these materials is associated with stopping the Li intercalation process in the two-phase region due to crystallographic domain disordering and, hence, blocking the completion of poorly reversible and kinetically complicated structural transformation of $Li_{1+x}V_3O_8$ into the high-lithiated structural modification.

Acknowledgements

The authors are indebted to Dr. Serge V. Pushko for the fruitful discussion and to J. Garden (INPG, Grenoble) for taking SEM micrographs.

References

[1] D.G. Wickham, J. Inorg. Nucl. Chem. 27 (1965) 1939.
[2] J.-M. Tarascon, M. Armand, Nature 414 (2001) 359.
[3] L.A. De Picciotto, K.T. Adendorff, K.T. Liles, M.M. Thackeray, Solid State Ionics 62 (1993) 297.
[4] S. Jouanneau, A. Verbaere, D. Guyomard, J. Solid State Chem. 178 (2005) 22.
[5] J. Kawakita, T. Miura, T. Kishi, J. Power Sources 83 (1999) 79.
[6] J. Kawakita, T. Miura, T. Kishi, Solid State Ionics 118 (1999) 141.
[7] J. Kawakita, T. Miura, T. Kishi, Solid State Ionics 120 (1999) 109.
[8] G. Pistoia, S. Panero, M. Tocci, R. Moshtev, V. Manev, Solid State Ionics 13 (1984) 311.
[9] G. Pistoia, M. Pasquali, M. Tocci, V. Manev, R. Moshtev, J. Power Sources 15 (1985) 13.
[10] J. Kawakita, T. Kato, Y. Katayama, T. Miura, T. Kishi, J. Power Sources 81-82 (1999) 448.
[11] G. Pistoia, M. Pasquali, G. Wang, J. Electrochem. Soc. 137 (1990) 2365.
[12] P. Novak, W. Scheifele, O. Haas, J. Power Sources 54 (1995) 479.
[13] K. West, B. Zachau-Christiansen, S. Skaarup, Y. Saidi, J. Barker, I.I. Olsen, R. Pynenburg, R. Koksbang, J. Electrochem. Soc. 143 (1996) 820.
[14] J. Xie, J. Li, H. Zhan, Y. Zhou, Mater. Lett. 57 (2003) 2682.
[15] J. Gao, C. Jiang, C. Wan, J. Power Sources 125 (2004) 90.
[16] H.Y. Xu, H. Wang, Z.Q. Song, Y.W. Wang, H. Yan, M. Yoshimura, Electrochim. Acta 49 (2004) 349.
[17] G.Q. Liu, C.L. Zeng, K. Yang, Electrochim. Acta 47 (2002) 3239.
[18] Q. Liu, H. Liu, X. Zhou, C. Cong, K. Zhang, Solid State Ionics 176 (2005) 1549.
[19] N. Kosova, E. Devyatkina, Solid State Ionics 172 (2004) 181.
[20] J. Kawakita, Y. Katayama, T. Miura, T. Kishi, Solid State Ionics 110 (1998) 199.
[21] G.Q. Liu, N. Xu, C.L. Zeng, K. Yang, Mater. Res. Bull. 37 (2002) 727.
[22] S. Jouanneau, A. Verbaere, S. Lascaud, D. Guyomard, Solid State Ionics 177 (2006) 311.
[23] Yu.D. Tretyakov, N.N. Oleinikov, O.A. Shlyakhtin, Cryochemical Technology of Advanced Materials, Kluwer Academic Publishers, 1997, pp. 162–185.
[24] S. Denis, E. Baudrin, F. Orsini, G. Ouvrard, M. Touboul, J.-M. Tarascon, J. Power Sources 81–82 (1999) 79.
[25] E. Baudrin, S. Denis, F. Orsini, L. Seguin, M. Touboul, J.-M. Tarascon, J. Mater. Chem. 9 (1999) 101.
[26] E.G. Gillan, R.B. Kaner, Chem. Mater. 8 (1996) 333.